

# QUANTIFYING MAGNETIC RECONNECTION AND THE HEAT IT GENERATES

Dana Longcope

*Department of Physics, Montana State University, Bozeman, MT 59717*

## ABSTRACT

Theories have long implicated magnetic reconnection in many aspects of coronal activity including the general process of coronal heating. Magnetic reconnection is fundamentally a change field line topology resulting from some non-ideal term in the generalized Ohm's law. Such a non-ideal effect may dissipate energy directly, or it may not, but it will topologically change field lines at a rate proportional to the integrated electric field,  $\dot{\Phi}$ . In any model where magnetic reconnection heats the corona the heating rate will scale with this rate of reconnection. We find that the observed scaling between heating power and reconnection rate is consistent with models where photospheric motions stress the coronal fields quasi-statically and reconnection releases the energy suddenly, but does not necessarily dissipate it. Such models are, in particular, consistent with the observation that X-ray luminosity of a structure scales almost linearly with the magnetic flux of that structure.

Key words: Magnetic reconnection.

## 1. INTRODUCTION

Models for heating the solar corona are typically designated as either AC or DC according to the frequency range of the photospheric Poynting flux. AC models consider frequencies at or above the fundamental frequency of coronal oscillation (Ionson, 1984), so that the Poynting flux is essentially carried by waves. DC models, on the other hand, consider the work done by the slowly varying component of the Poynting flux. These describe slow photospheric motions stressing the coronal field — adding free energy by increasing its current density. This process reaches a steady state, or at least a statistical steady state, when some form of magnetic reconnection manages to release energy at the same rate the stressing is adding it.

In addition to dissipating energy, magnetic reconnection changes the topology of magnetic field lines. The rate at which field lines are topologically changed is quantified by flux transfer rate  $\dot{\Phi}$ . The proposition that magnetic reconnection, rather than say wave dissipation, heats the corona is tantamount to the contention that the heating power  $P_h$  scales somehow with the rate of reconnection

$$P_h = C \dot{\Phi}^\mu, \quad (1)$$

where  $\mu > 0$ . Such a scaling would not apply to heating by high-frequency waves, even if they were Ohmically dissipated, since then dissipation occurs during both

phases of an oscillation, while flux transfer cancels over each period.

The present work reviews the different DC heating models, and finds that they may be further classified according to whether the magnetic reconnection heats the corona directly or indirectly. In direct models Ohmic dissipation converts magnetic energy into heat. In indirect heating models reconnection converts magnetic energy into some non-thermal form, such as kinetic energy or wave energy, which is then converted into heat more slowly than the reconnection. The two types of models predict different relationships between the heating rate and the magnetic reconnection rate. (i.e. different exponents  $\mu$  in relation [1]). The form of the heating which is actually in effect may be determined, in principle, by independently quantifying the reconnection rate  $\dot{\Phi}$  and heating rate  $P_h$ . The scaling of indirect heating mechanisms appear consistent with the data presently available.

## 2. RECONNECTION HEATING MODELS

Magnetic reconnection was first suggested as a possible mechanism for coronal heating by Parker (1972), in what amounted to the first DC heating model. According to his theory of topological dissipation, almost any motion of the photospheric surface would tend to generate topological discontinuities in the coronal field. The efficacy of such discontinuities at converting magnetic energy to heat was investigated in detail by Tucker (1973) and Levine (1974). Van Ballegooijen (1985) later suggested that smooth photospheric motions might not generate tangential discontinuities, but would instead produce magnetic structure of rapidly decreasing scales. In either scenario the generation of small magnetic length scale,  $\ell$ , would sufficiently diminish the dissipation time  $\tau_d = \ell^2/\eta$ , that it would match the photospheric driving time  $\tau_p$ . At this point the energy supplied by photospheric motion would be directly dissipated in the corona as heat. These are all forms of directly dissipative (or direct) DC heating models.

In any such model the coronal plasma is heated directly through Ohmic dissipation which is quadratic in the resistive electric field:  $Q = E^2/\eta$ . If the resistive electric field is also responsible for changing magnetic field topologies, as is fundamental to magnetic reconnection, then the rate of topological change,  $\dot{\Phi}$  will be linearly proportional to the electric field in some sense. The heating power from Ohmic dissipation will therefore scale

quadratically with  $\dot{\Phi}$ :

$$P_h = \frac{\dot{\Phi}^2}{R} \sim P_\eta, \quad (2)$$

where the constant of proportionality is dimensionally the inverse of a resistance. The net resistance  $R$  will naturally depend on the local resistivity  $\eta$  as well as on the magnetic field geometry. We refer to all models where the heating power scales quadratically with flux transport as *dissipative models*.

Heyvaerts and Priest (1984) proposed a coronal heating model which invoked magnetic reconnection in a fundamentally different role. They proposed that the coronal magnetic field was slowly stressed by photospheric motions, up to instants where it abruptly relaxed, releasing its stored energy. The relaxation they proposed occurred through reconnection at numerous unspecified sites, and terminated ultimately in the Taylor state of minimum energy at constant helicity (Taylor, 1974): it was Taylor relaxation. The energy released  $\Delta W$  would be the difference in equilibrium energies of the states before and after relaxation. The basic scenario was of quasi-static equilibrium punctuated by sudden relaxation. A variant of this basic scenario, quasi-static evolution punctuated by punctuated relaxation, was proposed by Longcope (1996) in three dimensions and Aly and Amari (1997) in two. In each of these the photospheric stressing produced magnetic equilibria containing tangential discontinuities (current sheets) which did not directly heat the corona, as Parker had first proposed, but instead stored free magnetic energy. They proposed that these current sheets would occasionally undergo fast magnetic reconnection thereby releasing the energy they stored. This scenario, dubbed *stick-slip reconnection* by Longcope (1996), relied on reconnection which was much faster than the stressing,  $\tau_{rx} \ll \tau_p$ , but which was inactive most of the time.

This class of models, to be called *quasi-static models*, differ from dissipative models by assuming that the magnetic reconnection time is far smaller than the photospheric driving time. The reconnection is only a means by which stored magnetic energy is liberated and need not correspond with the means by which it is dissipated.

The general scenario of short energy release following quasi-static build-up has come to be termed “nanoflaring” following Parker (1988). In this seminal paper predicting the small energy releases Parker actually proposed them not as an energy release but as an energy dissipation mechanism; the model was proposed as a time-variable version of his earlier topological dissipation model (Parker, 1972). It was subsequently shown that the hypothesized nanoflares could also explain the puzzling form of the corona’s differential emission measure (Sturrock *et al.*, 1990; Cargill, 1994). In spite of their wide-spread use in solar modeling, conclusive evidence that these small energy releases ( $\Delta W \sim 10^{23}$  erg) occur at all is still being sought. The present work focuses on discriminating between the possible roles of reconnection in coronal heating and will discuss nanoflares no further.

By definition punctuated reconnection transfers flux in discrete parcels  $\Delta\Phi$  at intervals  $\Delta t$ . Averaging over numerous individual events leads to an average rate of flux transfer rate  $\dot{\Phi} = \langle \Delta\Phi/\Delta t \rangle$ . In quasi-static models the heating rate is proportional to the energy *release* rate which must be linear in flux transfer

$$P_h = I_{qrx} \dot{\Phi}, \quad (3)$$

where the constant of proportionality has units of current. This scaling is a straightforward consequence of the assumed quasi-static nature, according to which the net energy liberated will depend only on the net flux transferred regardless of how infrequently the transfers occurred (i.e. both  $\dot{\Phi}$  and  $P_h$  will be inversely proportional to the event interval  $\Delta t$ ).

Quasi-static models invoke reconnection as a means of flux transfer but not of energy dissipation. While this leaves unanswered the issue of energy dissipation, it makes testable predictions about both the rate and locations of magnetic energy liberation. It is possible to discriminate between these two classes of reconnection heating models, dissipative and quasi-static, if we can independently measure both the rate of reconnection  $\dot{\Phi}$  and the heating power  $P_h$ . While the flux transfer rate  $\dot{\Phi}$  is only incidentally related to heating in dissipative models it seems unlikely that we might measure both the heating rate and the Ohmic dissipation rate in the solar corona *independently*. We review below several methods for measuring or inferring the flux transfer rate and comparing it to the heating rate.

### 3. RELATION TO RECONNECTION THEORIES

The possible independence of flux transfer and energy dissipation in a reconnection process seems more natural today than it did at the time dissipation heating models were first proposed. Early models of magnetic reconnection considered uniform magnetic diffusivity  $\eta$  to be the most likely mechanism for both flux transfer and dissipation. Sweet and Parker (Sweet, 1958a; Parker, 1957) found that reconnection at a current sheet proceeded at a rate scaling with the diffusion coefficient as  $\dot{\Phi} \sim \eta^{1/2}$ . This was recognized to be very slow under coronal conditions, unless the diffusivity was somehow enhanced.

It is noteworthy, however, that both flux transfer and dissipation occur at proportional rates in Sweet-Parker reconnection. According to the Sweet-Parker model, the self-consistent current sheet has a thickness  $\delta \sim \eta^{1/2}$ , while its length  $L$  (typically in the ignorable direction) and width  $w$  are set by global geometry. The total resistance of such a current sheet is therefore  $R = \eta L/w\delta \sim \eta^{1/2}$ . Since the effective resistance scales with reconnection rate,  $R \sim \dot{\Phi}$ , eq. (2) gives power dissipation  $P_\eta \sim \dot{\Phi}$  for a single Sweet-Parker current sheet. Both flux transfer and energy dissipation thus proceed at disappointingly small rates.

An illuminating counter-example is found in the flux pile-up regime observed in simulations of two-dimensional coalescence instabilities (Biskamp and Welter, 1980; DeLuca and Craig, 1992; Rickard and Craig, 1993). In their non-linear regime these simulations exhibit current sheets with magnetic field strength at their edges,  $B_s$ , locally enhanced by a factor scaling inversely with resistivity:  $B_s \sim \eta^{-q} B_0$ . Sweet-Parker scaling using the enhanced Alfvén speed yields a current sheet thickness  $\delta \sim \eta^{(q+1)/2}$  and a peak current density  $J \sim \eta^{-(3q+1)/2}$ . The flux transfer across this narrower current sheet,  $\dot{\Phi} \sim \eta^{(1-3q)/2}$ , scales as a lower power of resistivity than classic Sweet-Parker scaling ( $q = 0$ ), becoming genuinely fast (independent of resistivity) at the value  $q = 1/3$ . Numerical simulations do in fact show a peak flux transfer rate which is approximately *independent* of resistivity (Biskamp and Welter, 1980), suggesting a flux pile-up parameter  $q \simeq 1/3$ .

The total total resistance of the thinner current sheet is  $R \sim \eta^{(1-q)/2}$ , yielding an Ohmic dissipation power  $P_\eta \sim \eta^{(1-5q)/2}$ . For anything other than classic Sweet-Parker (i.e. for  $q \neq 0$ ) flux transfer and Ohmic dissipation scale as different powers of resistivity and thus would be unlikely to be proportional in a particular situation. For values  $q > 1/5$ , which includes that from numerical simulations, heating power scales *inversely* with resistivity, suggesting that such flux pile-up mechanisms would quickly exhaust all free-energy before achieving significant flux transfer (Craig *et al.*, 1993). The enhanced current sheet in coalescence simulations results from the collision between the islands. The faster reconnection appears to stall when this initial kinetic energy has been dissipated.

In order to explain fast magnetic flux transfer, for which there is ample evidence in solar flares, it was deemed necessary to eliminate the global current sheet which had been recognized as the obstruction to the outflows. Petschek (1964) proposed one scheme where plasma acceleration occurred at four slow shocks linked to a magnetic X-point. The slow-mode shocks were an alternative to the constrictive current sheet, and the reconnection proceeded at a much more acceptable rate since it scaled as  $\sim 1/|\ln(\eta)|$ . Unfortunately, numerical simulations using uniform diffusivity did not show Petschek-like reconnection, but exhibited instead the spontaneous formation of the troublesome current sheets along with the slow Sweet-Parker reconnection rate they demanded (Biskamp, 1986).

Several numerical simulations had in fact exhibited Petschek reconnection structure, but all had invoked a magnetic diffusivity enhancement within a small region (Ugai and Tsuda, 1977; Scholer and Roth, 1987), often through an assumed current-density dependence in the anomalous resistivity. Other studies of reconnection under collisionless conditions had used a generalized Ohm's law containing terms such as electron inertia or the Hall term, which transferred flux but without significant energy dissipation. In a remarkable series of simulations Birn *et al.* (2001) showed that various collisionless mech-

anisms, or combinations thereof, led to the spontaneous development of an X-type geometry similar to Petschek's and also to fast magnetic reconnection.

It has been recently recognized that these models and those collisional models using locally enhanced diffusivity produce fast reconnection for the same underlying reason: they break the frozen-flux law only in a small region (Erkaev *et al.*, 2000; Kulsrud, 2001; Biskamp and Schwarz, 2001). It turns out that fast reconnection is inconsistent with spatially uniform diffusion, but will happen naturally whenever the local rate of diffusion, or any other non-ideal field line transport, is locally enhanced. The degree of enhancement is not nearly as important as its localization (Biskamp and Schwarz, 2001).

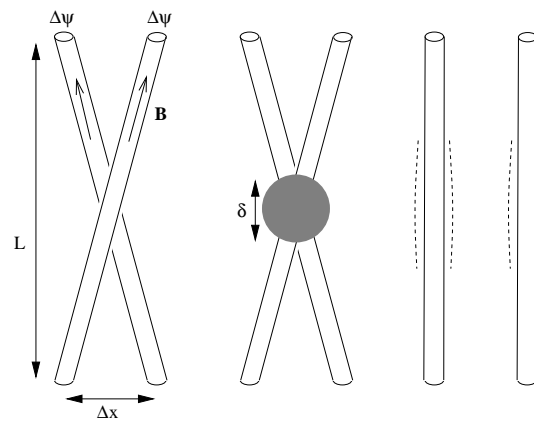


Figure 1. Schematic of localized reconnection occurring with a ball of diameter  $\delta$ .

Localization has the effect of changing reconnection from a dissipative to a flux-transfer process, which has profound significance for coronal heating models. It is possible to topologically change a significant number of field lines as they pass through a small region since they are one-dimensional curves. Consider the field lines advected by Alfvénic reconnection flow through a ball of very small diameter  $\delta$ . Flux will pass through this ball at a rate  $\dot{\Phi} \sim \delta B v_A$ . The current density within the ball will be  $J \sim B/\delta$ , and the electric field  $E \sim \dot{\Phi}/\delta$ . Integrating the Ohmic dissipation rate  $EJ$  over the volume gives dissipation power

$$P_\eta \sim EJ\delta^3 \sim B^2 v_A \delta^2 \sim v_A^{-1} \dot{\Phi}^2 ,$$

consistent with eq. (2). Localized reconnection is therefore much more efficient at flux transfer than at energy dissipation:  $\dot{\Phi} \sim \delta$  whereas  $P_\eta \sim \delta^2$ . The heart of the problem is that small-scale structures can dissipate only a small amount of energy even as they globally change the magnetic topology.

Localized reconnection can liberate magnetic field energy at the same rate it transfers flux, even though it

cannot dissipate energy so rapidly. Figure 1 shows two tubes each of flux  $\Delta\psi$  which are reconnected by resistivity confined to a ball. The dissipation will decrease the magnetic energy by as much as  $\Delta W_\eta \sim \Delta\psi^2/\delta$ , the free energy within the ball. By changing the footpoints of the tubes, however, the reconnection permits each to become shorter thereby reducing the overall equilibrium magnetic energy by  $\Delta W \sim B\Delta\psi\Delta x^2/L$ . For very small flux tubes this far exceeds the power dissipated in the reconnection process so there will be kinetic energy left after the reconnection. It is the dissipation of this kinetic energy which will ultimately provide heating. The salient point is that the localized reconnection *released* the magnetic energy rapidly, but could not dissipate it.

Detailed physical support for these estimates can be found in a number of fully dynamic, two-dimensional calculations of non-steady reconnection localized in space (Semenov *et al.*, 1983; Biernat and Heyn, 1987; Heyn and Semenov, 1996; Semenov *et al.*, 1998; Nitta *et al.*, 2002). All of these calculations begin with an infinitesimally thin current sheet separating two layers of uniform, opposing field (see fig. 2). They follow the ideal ( $\eta = 0$ ) external response to fast reconnection occurring at a single point on the sheet (or very small region) with the prescribed time-dependent rate  $\dot{\Phi} = E(t)L$ , switched on at some time  $t_0$ . In spite of the time-dependence, the central region resembles the steady-state Petschek configuration with four slow mode shocks linked to the reconnection site. Due to the sudden turn-on, however, the shock structures are finite and enclose “bubbles” of much weaker field and bulk flow velocity  $\sim v_A$  (see fig. 2). Since the non-ideal electric field is confined to the small region on the current sheet, the slow shocks do not dissipate any energy, but they do convert free magnetic energy to kinetic energy to form the bubbles (Semenov *et al.*, 1998).

Even if magnetic reconnection ceases (see bottom panel of fig. 2) the slow shocks and the bubbles they enclose continue traveling outward at the Alfvén speed. Two bundles of flux  $\Delta\Phi = \int \dot{\Phi} dt$  were broken and reconnected to form hair-pin shaped post-reconnection tubes; these are the analogs of the flux tubes in fig. 1. Immediately following the reconnection magnetic tension at the curves of post-reconnection hair-pins causes a rapid retraction. As they retract the overall magnetic energy decreases and the kinetic energy increases (the bubbles continue sweeping up mass, Semenov *et al.*, 1998). The total magnetic energy ultimately released will depend on the anchoring of the reconnected field lines far from the reconnection site (this was also the case in the simple cartoon of fig. 1). If the field finds a new equilibrium, after dissipating the kinetic energy of the bubbles, it will be lower than the initial energy by some amount  $\Delta W \sim \Delta\Phi$  proportional to the net reconnected flux. Thus the energy *released* by the reconnection depends on the net flux transferred and on global parameters but not on the reconnection rate; in contrast, the energy *dissipated* by reconnection does depend on the reconnection rate and will be must smaller owing to its localization.

The foregoing examples serve to illustrate the relationship between flux transfer  $\Delta\Phi$  and magnetic energy release  $\Delta W$  in several simple geometries. The relationship has been generalized to three-dimensional coronal geometries of arbitrary complexity by Longcope (2001) in the theory of flux constrained equilibria (FCE). A three-dimensional coronal field of arbitrary complexity can transfer flux at each of its magnetic separators so flux transfer is quantified by a vector  $\Delta\psi_i$ . The free energy of a given equilibrium will be a function of the fluxes presently enclosed by each of the separators,  $W(\psi_i)$ . Small flux transfers across various separators will change the total energy by

$$\Delta W \simeq \sum_i \frac{\partial W}{\partial \psi_i} \Delta \psi_i . \quad (4)$$

This is the generalization, to arbitrary coronal geometry, of the  $\Delta W \sim \Delta\Phi$  proportionality described above.

The energies  $\Delta W \sim \Delta\Phi$  liberated by successive fast releases produce a time-averaged power  $P_h = \langle \Delta W / \Delta t \rangle \sim \dot{\Phi}$ , as a natural consequence of the punctuated quasi-static process. This power must match the averaged heating rate but will far exceed the Ohmic dissipation rate  $P_h \gg P_\eta \sim \dot{\Phi}^2$ .

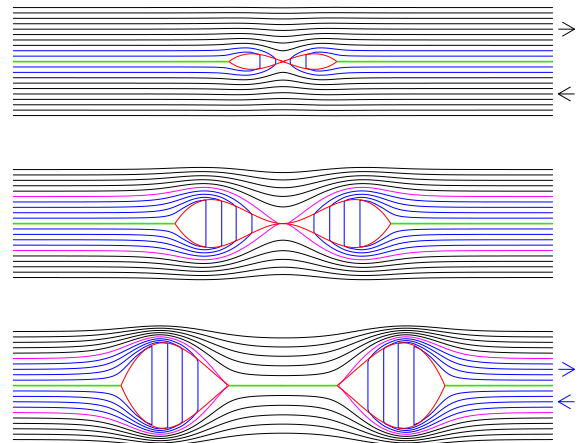


Figure 2. The time-dependent solution of Biernat and Heyn (1987) at three successive times proceeding from top to bottom. Uniform layers of opposite field (black) are separated by an infinitesimally thin current sheet (green). Reconnection occurs at a small region at the center of the current sheet, creating hair-pin shaped reconnected field lines (blue), bounded by separatrices (magenta). The reconnection pulse persists only through the time of the middle panel, so a central section of current sheet has reformed by the time of the bottom panel. Slow shocks (red) extend outward from the reconnection site, while reconnection occurs. The slow shocks enclose two bubbles of approximately vertical reconnected field which propagated away from reconnection site at the down-stream Alfvén speed.

#### 4. OBSERVATIONAL CONSTRAINTS

Reconnection heating mechanisms may be classified according to how the heating rate scales with the flux transfer rate. Which category of mechanism is actually at work may therefore be observationally determined by measuring the heating rate and the flux transfer rate independently. A review by Withbroe and Noyes (1977) summarized the state of knowledge by listing heat fluxes,  $F_h$  [erg sec<sup>-1</sup> cm<sup>-2</sup>] for each of three generic portion of the corona: active region, quiet Sun and coronal hole. These values remain an important constraint on coronal heating mechanisms today.

There has traditionally been less effort devoted to measuring the rate at which magnetic field lines are reconnected. In order to even make sense of this quantity one must ascertain which field lines are being topologically changed. Posed more concretely, “Which two kinds of field lines are being destroyed and which two kinds are being created?” Only when that is known can one hope to measure the rate at which this flux transfer takes place.

The most well-known measurements of this kind were made for the reconnection following two-ribbon flares. The reconnection is thought to occur in the wake of an eruption, converting newly opened field lines, rooted in each polarity, into one closed field line inter-linking the polarities and one field line open at both ends. According to this picture, the chromospheric ribbons mark the boundary between pre-reconnection and post-reconnection field lines. The progress of the ribbons across the photosphere is equivalent to the reconnection rate  $\dot{\Phi}$ . Fletcher and Hudson (2001) tracked the ribbons of the 2000-July-14 flare, observed in the 195 Å images of TRACE, across a magnetogram from SOHO MDI. This yielded reconnection rates of  $\dot{\Phi}$  between  $5 \times 10^{16}$ – $20 \times 10^{16}$  Mx/sec (500 MV – 2,000 MV) for the period following the flare. A troubling aspect of the observations was that measurements from each polarity, which should in principle agree, differed by more than a factor of two (Fletcher and Hudson, 2001).

When considering reconnection in non-flaring contexts it becomes even more difficult to establish observationally which field lines are being reconnected. Indeed, there is a limit to the level of detail with which we can determine the topology of coronal magnetic field lines at all. We are therefore restricted to measuring the flux transfer rate in cases with clearly distinguishable topological classes of field lines. The cases where these distinctions may be most clearly made are those with footpoints lying in distinct photospheric flux concentrations, hereafter called *sources*.

The topological theory of coronal field anchored in distinct photospheric source regions, called *Magnetic Charge Topology*, has been developed by numerous authors beginning with Sweet (1958b), Baum and Bratenahl (1980) and Gorbachev *et al.* (1988). A general quantitative theory has been developed by Longcope in a series of papers (Longcope, 1996, 2001; Longcope and Klap-

per, 2002). Domains of distinct field lines are separated by magnetic separatrices which are the fan surfaces of magnetic null points. Most null points lie in the photospheric areas, surrounding the source regions, which are assumed to have no vertical field ( $B_z = 0$ ). The separatrices intersect along a network of separators, which are each individual field lines when the coronal field is smooth, but become current sheets in more general cases (Longcope, 2001).

The allocation of fluxes in all domains can be found from the flux in each source region and the integrated flux through each closed separator loop (Longcope and Klapper, 2002). It follows that any change in domain fluxes must occur either through emergence or separator reconnection. Neglecting for the moment possible emergence through the photosphere, the rate at which flux in domain  $i$  changes is proportional to the loop voltage on one or more separators which enclose it. It is this loop voltage which may be determined both theoretically and, in some cases, observationally.

##### 4.1 The general scaling law

Considered in general, coronal heating provides some generic portion of the atmosphere with a volumetric heating rate  $Q$ . The only way to define a flux transfer rate  $\dot{\Phi}$  in such a vague setting is to posit a time  $\tau_{\text{rcyc}}$  in which a typical field line is reconnected once. Within a region of net flux  $\Phi$  the flux transfer rate will be on average  $\dot{\Phi} = \Phi/\tau_{\text{rcyc}}$ . The heating attributable to magnetic reconnection should scale linearly or quadratically with this in the quasi-static and dissipative models respectively

$$P_h = \begin{cases} \Phi I_{\text{qrx}}/\tau_{\text{rcyc}} & , \quad \text{quasi-static} \\ \Phi^2/(R\tau_{\text{rcyc}}^2) & , \quad \text{dissipative} \end{cases} \quad (5)$$

Schrijver *et al.* (1985) and Schrijver *et al.* (1989) reported different flux-flux relations which combine to yield a nearly linear relation between photospheric magnetic field strength and X-ray flux ( $F_x \sim B^{1.1}$ , see Schrijver and Zwaan, 2000). More recently, Pevtsov *et al.* (2003) produced a composite data set recording soft X-ray luminosity,  $L_x$  (over the band-pass 2.8–36.6 Å), and total flux  $\Phi$  for various magnetic structures spanning more than fourteen orders of magnitude in  $\Phi$ . The composite data set includes coronal bright points (Longcope *et al.*, 2001), active regions (Fisher *et al.*, 1998), the Sun as a star and T-Tauri stars. They found X-ray luminosity was fit by the relationship

$$L_x \simeq 1.2 \times 10^{24} \text{ erg/sec} \times \left( \frac{\Phi}{10^{21}} \right)^{1.15} , \quad (6)$$

particularly well for all solar structures.

Making the further assumption that X-ray luminosity over the observed pass band is proportional to net coronal heating power,  $L_x \simeq \chi P_h$ , implies that heating power

scales almost linearly with flux as predicted by quasi-static models. The data implies that the combinations of proportionality constants,  $\chi I_{\text{qrx}}/\tau_{\text{cyc}}$  is approximately equal to  $10^3 \text{ erg sec}^{-1} \text{ Mx}^{-1} = 10^4 \text{ A/sec}$  almost independent of  $\Phi$ . It is also possible to explain this relationship with dissipative models, provided the product of constants  $R\tau_{\text{cyc}}^2$  scales almost linearly with the total flux of the feature. We show below how a theoretical model which can explain the former scaling.

The constant  $\chi$  may be found by comparing relation (6) to the heat flux reported by Withbroe and Noyes (1977) in their review:  $F_h = 3 \times 10^5 \text{ erg/sec/cm}^2$  in the quiet Sun. The corona of the quiet Sun is primarily structured by the network flux elements whose average unsigned flux density was reported to be  $\langle |B_z| \rangle = 1.5 \text{ Mx/cm}^2$  by Schrijver *et al.* (1997).<sup>1</sup> Using this flux density in the scaling of Pevtsov *et al.* (2003) gives a soft X-ray flux of  $F_x = 2 \times 10^3 \text{ erg sec}^{-1} \text{ cm}^{-2}$  for a generic quiet Sun region. Dividing this by the heating power (Withbroe and Noyes, 1977) we deduce that the soft X-ray luminosity accounts for  $\chi = F_x/F_h = 0.0067$  of the total heating power. Withbroe and Noyes (1977) estimate that only one-third of the deposited heat is radiated ( $F_r = 10^5 \text{ erg sec}^{-1} \text{ cm}^{-2}$ ) while the remaining two-thirds is conducted downward. Our ratio indicates that  $3\chi \simeq 2\%$  of the quiet Sun radiation occurs within the bandpass of 2.8–36.6Å used by Pevtsov *et al.* (2003); this is not unreasonable for a plasma at about one to two million Kelvins (Loren Acton, private communications).

Dividing the observed trend by the value of  $\chi$  inferred above gives reconnection heating constant  $I_{\text{qrx}}/\tau_{\text{cyc}} = 1.4 \times 10^6 \text{ A/sec}$ . This value appears to vary only slightly with the size of the magnetic structure involved. As a further check, we note that the flux density typical of plage,  $\sim 100 \text{ Mx/cm}^2$ , predicts a heat flux of  $F_h \sim 1.4 \times 10^7 \text{ erg sec}^{-1} \text{ cm}^{-2}$ , consistent with the value expected in an active region (Withbroe and Noyes, 1977).

## 4.2 Quiet Sun recycling time

An observational study by Close *et al.* (2004) estimates the field line recycling times scale  $\tau_{\text{cyc}}$  in the quiet Sun to be roughly 2 hours. They identified photospheric sources in each of 50 high-resolution MDI magnetograms of disk-center quiet Sun, made at a 15-minute cadence. The flux  $\Phi_a$  and centroid location is determined for each source region above a threshold magnetic field. A potential field is extrapolated from point sources with matching fluxes and locations. Randomly selected field lines are integrated from each source within the 80 Mm  $\times$  80 Mm central region in order to determine the fluxes  $\psi_i$  in each of their interconnecting domains. The interconnecting flux must relate to the photospheric flux according to the balance law  $\Phi_a = \sum_i M_{ai}\psi_i$ , where the incidence matrix  $M_{ai}$  is

<sup>1</sup>There is at least an order of magnitude more flux in intranetwork fields (Lin and Rimmele, 1999; Lites, 2002), but since this is mixed and structured on very fine scales, it will not contribute flux to coronal heights. Recent work has shown that the intranetwork field will contribute *field lines* (Schrijver and Title, 2003), affecting the topology, but this does not change the net flux at coronal heights.

unity if domain  $i$  connects to source  $a$  and zero if it does not (Longcope, 2001).

The rates of flux change,  $\dot{\Phi}_a$  and  $\dot{\psi}_i$ , in time-evolving potential field can be determined by associating sources between successive magnetograms and repeating the procedure above for each time. Any change in the photospheric flux,  $\dot{\Phi}_a$ , must occur through emergence or submergence across the photosphere. The ratio  $|\dot{\Phi}_a/\dot{\Phi}_a|$  gives characteristic time over which source flux will be changed; a time-scale for emergence/submergence. Averaging this over all sources Close *et al.* (2004) find a time-scale for recycling the photospheric flux  $\sim 15$  hours, consistent with those from previous studies of quiet Sun flux elements (Hagenaar, 2001; Hagenaar *et al.*, 2003).

Changes in the source fluxes and source locations cause the domain fluxes  $\psi_i$  to vary in time. Since it is always possible to define an incidence matrix which is constant over a given interval, the flux changes must be related according to

$$\dot{\Phi}_a = \sum_a M_{ai}\dot{\psi}_i . \quad (7)$$

Changes due to coronal reconnection alone,  $\dot{\psi}_i = R_i$ , must be consistent with no photospheric changes at all,  $\sum_i M_{ai}R_i = 0$ . Any remaining changes must be attributed to the effects of emergence and submerge,  $S_i = \dot{\psi}_i - R_i$ .

The decomposition of  $\dot{\psi}_i$  into reconnection and emergence/submergence contributions cannot, however, be unique since the incidence matrix  $M_{ai}$  is almost always singular<sup>2</sup> (Longcope, 2001). Close *et al.* (2004) propose two different schemes for performing the decomposition, thereby yielding two estimates of the quiet Sun recycling time. In the first they time-average the source flux  $\dot{\Phi}_a$  between successive steps, so that  $\dot{\Phi}_a = 0$  and any observed domain flux changes must be due to reconnection alone. In the second they require all emergence or submergence to occur with a subset of domains (a minimum spanning tree) whose incidence matrix is invertible. They then solve for  $S_i$  from the observed  $\dot{\Phi}_a$ , and from this find the reconnection rate  $R_i = \dot{\psi}_i - S_i$ .

The two different methods described above lead to two different vectors  $R_i$  which lead in turn to recycling times of  $\tau_{\text{cyc}} = 3$  hours and  $\tau_{\text{cyc}} = 1.4$  hours respectively. The rough agreement between these different methods gives some confidence that the typical coronal recycling time in the quiet Sun corona is somewhere around 2 hours. This means that each photospheric footprint is connected, via coronal field, to about 8 different partners during its 15 hour life. If the heat for the quiet Sun corona can be attributed to reconnection then it must arise from effects of this frequent footprint swapping. The constant of proportionality for a 2-hour recycling time will be  $I_{\text{qrx}} = 10^6 \text{ A/s} \times \tau_{\text{cyc}} = 10^{10} \text{ Amps}$ . While it has

<sup>2</sup>The only exceptions are fields without separators, which are unlikely to occur in a realistic, complex field.

units of current, this is simply the constant relating reconnection rate to heating rate in the quiet Sun according to (3). We show below that in a geometric model this value does correspond to the current across which the reconnection has occurred.

### 4.3 X-ray bright points

X-ray bright points are small ( $\lesssim 40$  Mm) regions of coronal emission typically in coronal holes or regions of quiet Sun, almost always associated with pairs of opposite magnetic sources (Krieger *et al.*, 1971; Golub *et al.*, 1974, 1977). The coincidence between the coronal emission and magnetic sources has motivated several models in which bright points are heated by magnetic reconnection (Parnell *et al.*, 1994; Longcope, 1998). A survey by Longcope *et al.* (2001) found 285 bright points in EIT observations and matched them to bipoles in near-simultaneous MDI magnetograms. The net power heating the bright point,  $P_h$ , was calculated by matching the emissions in two EUV bands (171 Å and 195 Å) to an equilibrium loop model. This power turned out to be clearly correlated with the magnetic flux in the photospheric sources:  $P_h \sim 10^{24} \text{ erg/sec} (\Phi/10^{19} \text{ Mx})$ . A subset of the bright points were subsequently identified in Yohkoh images and used in the compilation of Pevtsov *et al.* (2003); they fill in the  $3 \times 10^{18} \text{ Mx} < \Phi < 10^{20} \text{ Mx}$  range of scaling (6). The ratio of the fits reported in these two papers give  $L_x/P_h \sim 0.01$ , corroborating the value of  $\chi$  deduced above.

A more recent survey by Aver *et al.* (2005) uses multiple five-minute-averaged MDI magnetograms, spanning three hours, to derive a relative velocity  $\mathbf{v}$  between the photospheric poles of each bright point. Poles separated by  $d$  and moving toward each other with radial velocity  $-v_r$  will collide in a time  $\tau = d/|v_r|$ . There are 54 converging bipoles, defined as those with relative velocity within  $70^\circ$  of the line of separation, whose average and median lifetimes are 23.9 and 11.9 hours respectively. Using the lifetime to estimate the reconnection rate  $\dot{\Phi} = \Phi/\tau$ , Aver *et al.* (2005) find a strong correlation with  $P_h$ , shown in fig. 3. The dashed line, marking a reconnection constant of  $I_{\text{qrx}} = 10^{11}$  Amps passes near the center of these points. It is noteworthy that the power is correlated far more strongly with the product  $\Phi|v_r|$ , and that a line defined by the constant of proportionality  $B_0 \simeq 10$  G lies underneath the majority of points.

## 5. SEPARATOR CURRENTS

### 5.1 The Minimum Current Corona Model

The Minimum Current Corona model (MCC, Longcope, 1996, 2001) provides a theoretical context in which the coronal heating constant  $I_{\text{qrx}}$  may be interpreted. When two opposing photospheric sources of flux  $\Phi_+$  and  $\Phi_-$  approach one another, as in an X-ray bright point, the coronal field lines interconnecting the two sources compose a domain with net flux  $\psi$ , enclosed by a separator (see fig. 4). The domain flux for a potential corona,  $\psi^{(v)}$ ,

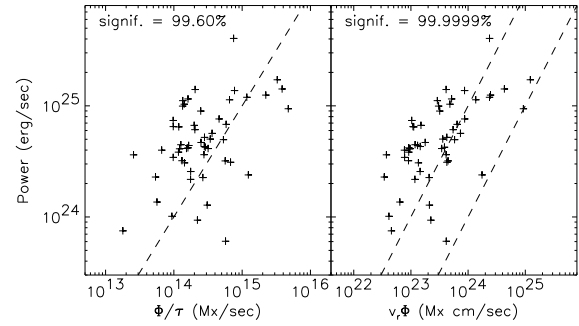


Figure 3. Data from a survey of EUV bright points with converging poles (Aver *et al.*, 2005). The left panel shows the heating power  $P_h$  vs. an estimate of the reconnection rate  $\dot{\Phi}$ . The dashed line shows the curve defined by  $I_{\text{qrx}} = 10^{11}$  Amps. The right panel shows  $P_h$  against the product  $\Phi|v_r|$ . The dashed line show  $B_0 \Phi|v_r|$  for  $B_0 = 1$  G (lower) and  $B_0 = 10$  G (upper). The significance listed at the top is from the Spearman rank order correlation statistic (Press *et al.*, 1986)

will naturally increase as the sources approach. This occurs through kinematic reconnection along the separator (Greene, 1988; Lau and Finn, 1990). The reconnection rate  $\dot{\psi}^{(v)}$  is the integrated electric field parallel to the separator field line (Sweet, 1958b; Longcope and Cowley, 1996).

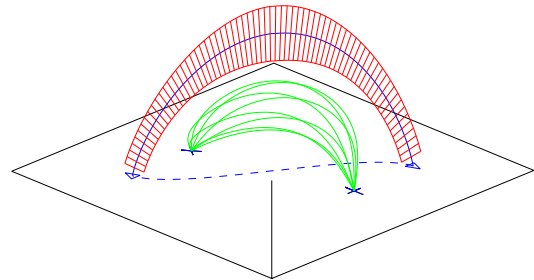


Figure 4. The MCC applied to a pair of converging sources, shown as blue crosses. Representative interconnecting field lines are shown in green. The blue solid line is the separator field line of the potential field, the dashed line closes the path along the photosphere. All interconnecting field lines must pass through this loop. The separator current sheet is indicated by red ribs.

A highly conducting plasma will not admit an electric field parallel to any coronal field line, even the separator field line, so  $\dot{\psi} = 0$  and the field cannot remain potential. The potential field is the one which minimizes the magnetic energy of the corona subject to the distribution of photospheric flux. Seeking a minimum subject to the additional constraint provided by the fixed interconnecting flux  $\psi$  yields the flux constrained equilibrium (FCE) defined by Longcope (2001). The Euler-Lagrange equation from the variation shows the equilibrium to be current-free everywhere except for a singular layer along the separator.

The transformation of the separator from a line in the potential field to a ribbon-like surface is analogous to the deformation of a two-dimensional potential X-point into a current sheet, first described by Green (1965) and later by Syrovatskii (1971). The Green-Syrovatskii current sheet is, in fact, the basic element of the FCE in two-dimensions (Aly and Amari, 1997; Longcope, 2001). A three-dimensional field linking  $S$  distinct photospheric sources by coronal field lines in  $D$  different domain will have at least  $D - S + 1$  separators all of which will be current sheets in the FCE (Longcope and Klapper, 2002).

The FCE can be constructed as the sum of the potential field and a field due to its separator current sheets. A separator of length  $L$  carrying a relatively small current  $I$  will generate a self-flux approximately (Longcope and Silva, 1998; Longcope and Magara, 2004)

$$\psi^{(\text{cr})} = IL \ln(eI^*/|I|) , \quad (8)$$

where  $e = 2.718$  is the base of the natural logarithm, and  $I^*$  is a parameter related to the average magnetic shear along the potential field's separator. In order to match the required domain flux, a field with a single current sheet must have a self-flux  $\psi^{(\text{cr})} = \Delta\psi \equiv \psi - \psi^{(\text{v})}$ . Inverting relation (8) yields the current  $I(\Delta\psi)$  in terms of the difference between the actual domain flux and that of a potential field from the present photospheric field distribution. As the photospheric field evolves so does  $\psi^{(\text{v})}$ , and hence  $\Delta\psi$ , which means the current grows. This is the nature of photospheric stressing in the minimum current corona model.

The imposition of flux constraints means that the FCE has an energy above that of the potential field (the absolute minimum) by

$$\Delta W_{\text{FCE}}(I) = \frac{1}{2} LI^2 \ln \left( \frac{\sqrt{e} I^*}{|I|} \right) , \quad (9)$$

(Longcope and Silva, 1998; Longcope and Magara, 2004). The actual coronal field will probably be subject to numerous constraints beyond that on its domain fluxes, such as on its helicity or the photospheric footpoints of specific field lines (line tying), so eq. (9) represent a lower bound on the free energy of the coronal field. It does, however, represent energy stored by that one constraint which will be eliminated by magnetic reconnection transferring flux across the separator. Other constraints, for example the helicity constraint, are far more robust and their associated energy will be less accessible to a heating mechanism. Thus  $\Delta W_{\text{FCE}}$  is a reasonable estimate of the energy release by separator reconnection.

The approaching sources from fig. 4, by generating a potential loop-voltage  $\dot{\psi}^{(\text{v})}$  will produce a separator current increasing at

$$\dot{I} = \left( \frac{\partial \psi^{(\text{cr})}}{\partial I} \right)^{-1} \dot{\psi}^{(\text{v})} \simeq L^{-1} \dot{\psi}^{(\text{v})} . \quad (10)$$

Reconnection triggered when the current reaches a threshold,  $|I| = I^{(\text{t})}$ , will occur after a delay  $\Delta t =$

$I^{(\text{t})}/|\dot{I}|$ . The repeated releases of energy  $\Delta W_{\text{FCE}}(I^{(\text{t})})$  at this interval will produce an average heating power

$$\langle P \rangle = \frac{\dot{I} \Delta W_{\text{FCE}}(I^{(\text{t})})}{I^{(\text{t})}} = I^{(\text{t})} \dot{\psi}^{(\text{v})} , \quad (11)$$

up to a ratio of logarithms of arguments proportional to  $I^*/I^{(\text{t})}$ . The repeated reconnection will keep  $\psi \simeq \psi^{(\text{v})}$ , so the average heating will be linear in the reconnection rate with a constant given by the reconnection threshold  $I_{\text{qrx}} = I^{(\text{t})}$ .

## 5.2 Observations

Kankelborg and Longcope (1999) and Longcope and Kankelborg (2001) studied TRACE observations of a bright point that appeared near disk center on 1998 June 17 (see fig. 5). Two poles, each of  $\simeq 1.1 \times 10^{19}$  Mx, separated by  $d = 11.3$  Mm approach one another at  $\dot{d} = -218$  m/sec. After the subtracting observed submergence rate,  $S = 3.5 \times 10^{14}$  Mx/sec, the vacuum reconnection rate was found to be  $\dot{\psi}^{(\text{v})} = 1.6 \times 10^{14}$  Mx/sec (1.6 MV). The MCC predicts that current will accumulate quasi-statically along the 25 Mm long separator at a rate  $\dot{I} = 6.4 \times 10^5$  Amps/sec.

The TRACE observations show a coronal loop interconnecting the converging poles. Matching to the magnetic model shows that the loop contains  $\Delta\psi \simeq 1.8 \times 10^{17}$  Mx (see fig. 5) — roughly 20 minutes of accumulated flux. If this represented all of the flux accumulated before reconnection then the threshold current would be only  $7.2 \times 10^8$  Amps; far less than needed to produce a heating power  $P \sim 10^{24}$  erg/sec typical of a bright point. Matching such a heating rate would require that  $6 \times 10^{10}$  Amps had accumulated on the separator *prior* to any reconnection. That is to say, significant reconnection did not occur for about  $\sim 26$  hours during which time the separator current sheet stored magnetic energy. Releasing this stored energy through fast reconnection would power the coronal bright point, although the dissipation of the energy would have to occur rather slowly to explain the observed life time of the bright point being far longer than a free cooling time (Longcope and Kankelborg, 2001).

A similar separator reconnection scenario, on a much larger spatial scale, was used by Longcope *et al.* (2005) to model reconnection between neighboring active regions. They studied the emergence of active region 9574 in the immediate vicinity of an existing active region (9570) over the course of two days (2001 Aug. 10–11). Observations by TRACE (171 Å, see fig. 6) and *Yohkoh* (SXT) show numerous coronal loops interconnecting the leading (negative) polarity of AR 9570 to the trailing (positive) polarity of AR 9574. Sequential magnetograms (MDI) show the polarities of 9574 begin emerging at 7:30 on Aug 10 at a rate  $S = 3.1 \times 10^{16}$  Mx/sec and separating at  $\dot{d} = 215$  m/sec (quite remarkably this is the same speed at which the tiny poles of the aforementioned XBP were converging). A magnetic model based on this data shows reconnection across the potential-field separator at  $\dot{\psi}^{(\text{v})} = 3.9 \times 10^{15}$  Mx/sec.

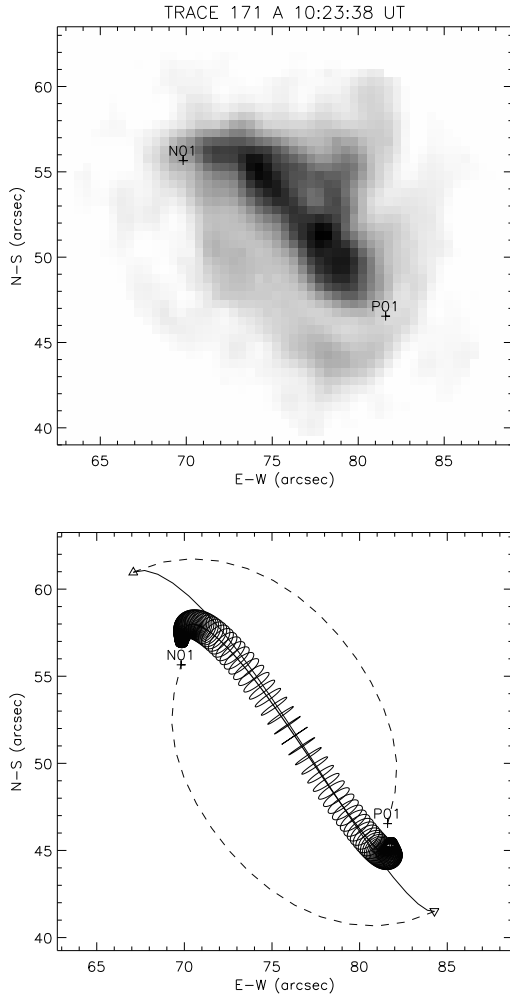


Figure 5. An EUV bright point studied by Kankelborg and Longcope (1999) and Longcope and Kankelborg (2001). Top panel is the background-subtracted TRACE 171 Å image. Bottom panel is the post-reconnection loop of  $\delta\psi = 1.8 \times 10^{17}$  Mx, from the magnetic model. Triangles are the photospheric null points, dashed lines are from their fan surfaces and the solid curve connecting them is the separator (Reproduced from Longcope and Kankelborg, 2001).

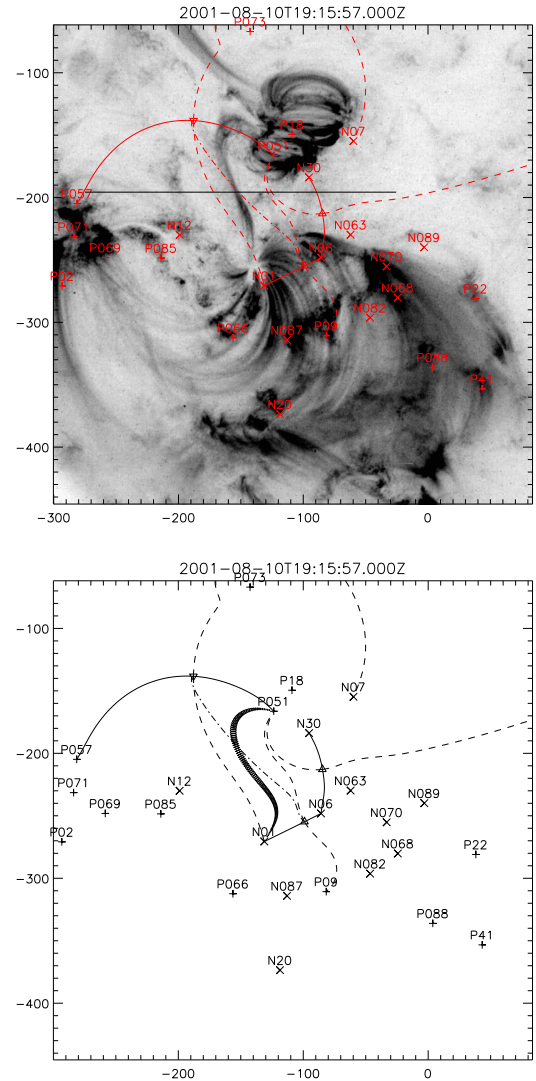


Figure 6. Active region AR9574 emerging to the North in the presence of existing active region AR9570 (South). Top panel shows a back-ground subtracted TRACE 171 Å image. Sources from the magnetic model are shown in red, along with the null points and the footprints of the separatrix surfaces. The horizontal black line was the line across which the interconnecting field lines were identified. The bottom panel shows features of the magnetic model along with a single post-reconnection flux tube of  $\Delta\psi = 5 \times 10^{17}$  Mx. (Reproduced from Longcope et al., 2005)

Interconnection loops were identified in the 41 hours of TRACE data using a horizontal strip separating the two active regions (see fig. 6). By summing up the cross sectional areas of all observed loops (assuming circular cross section) Longcope *et al.* (2005) estimate the actual reconnection. Assuming the observed loops have a ratio of field strength to filling factor of 65 G (the field strength in a potential fields is  $\sim 15$  G), and advancing the time-sequence 3 hours to account for post-reconnection cooling, they obtain the observed  $\psi(t)$  shown in fig. 7. It is notable that little reconnection occurs during the first 24 hours of emergence, in spite of the steady requirement for it in the potential field (i.e.  $\psi^{(v)}$ ). When the reconnection does occur it transfers a significant fraction of the accumulated flux (65 G was chosen to make it 100%) in only 3 hours, at a rate as large as  $\dot{\psi} = 2.5 \times 10^{16}$  Mx/sec = 260 MV. This coincides, after accounting for a 3-hour cooling delay, with a period of elevated X-ray emission (though not a flare) from which the GOES 1–8 Å band observed  $\Delta E = 7 \times 10^{28}$  ergs. In the MCC model the separator current has built to  $I = 3 \times 10^{10}$  Amps, after 24-hours of accumulation, storing an energy  $\Delta W_{\text{FCE}} = 4.5 \times 10^{29}$  ergs comfortably larger than the total observed in 1–8 Å X-rays. As in the coronal bright point, the post-reconnection loops remain bright much longer than the free cooling time. This suggests that the energy released by reconnection, perhaps transformed to waves or kinetic energy, was dissipated more gradually in the time following the reconnection (Longcope *et al.*, 2005).

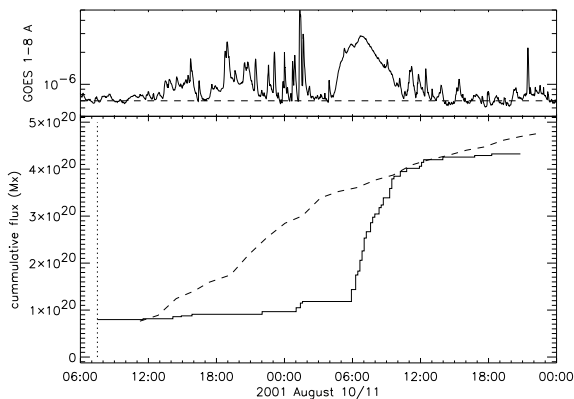


Figure 7. The flux interconnecting ARs 9574 to 9570. Bottom panel shows flux  $\psi^{(v)}$  (dashed) and the flux inferred from EUV images (solid). Top panel shows the disk-integrated SXR flux in GOES 1–8 Å band.

## 6. SUMMARY

This review has posited that coronal heating power, if it is generated by magnetic reconnection, must scale as some power of the rate  $\dot{\Phi}$  at which reconnection occurs. Those scalings arising from energy release after quasi-static stressing,  $P_h = I_{\text{qrx}} \dot{\Phi}$ , seem consistent with a wide variety of observational data. The constant of proportionality,  $I_{\text{qrx}}$ , has different interpretations in differ-

ent quasi-static models. In the Minimum Current Corona (MCC) model it represents the current along the separator at which the reconnection occurs.

A compilation of a wide variety of coronal structures indicates general heating at a rate proportional to the structure’s net flux. The constant of proportionality in this relationship suggests that  $I_{\text{qrx}}/\tau_{\text{rcyc}} \simeq 10^6$  Amps/sec, where  $\tau_{\text{rcyc}}$  is the typical time over which a field line in the structure is reconnected. Observations of particular X-ray bright points and active regions give different values of  $I_{\text{qrx}}$  ranging from  $10^{10}$  to  $10^{11}$  Amps, but the ratio seems to be relatively independent of size or structure, at least on the Sun.

The foregoing approach differs from the more traditional one of equating the heating flux,  $F_h = P_h/A$ , to the Poynting flux crossing the photosphere  $\mathbf{B} \times (\mathbf{v} \times \mathbf{B})/4\pi$ . Poynting flux is naturally related to the local magnetic field strength  $B_p$  and velocity  $v_p$  at the photosphere. The majority of heating modelers have consequently cast their results in these terms (Mandrini *et al.* (2000) presents a very thorough review of the most common models and the relationships they predict). This approach leads to no ambiguity in the majority of theoretical models, which use straight loops anchored to uniform photospheric field. There is considerably more ambiguity, however, when such scalings are applied to realistic magnetic regions. The quiet Sun, for example, is composed of very small magnetic elements of strong (500–1000 G) magnetic field, distributed primarily inside network cells with a filling factor of 1–2 % (Lin and Rimmele, 1999). Strict application of the Poynting-flux argument demands that the local value,  $B_p \sim 1000$  G, be used to compute the coronal heating. When considering an average heating flux, on the other hand, one might be justified in adopting the average unsigned flux density  $\bar{B}_p \sim 20$  G. In our approach of quantifying coronal reconnection rather than Poynting flux we conclude that only network elements, whose unsigned density is smaller by yet another order of magnitude, could heat the corona. This turns out to be the value consistent with the scaling law (6).

Observational evidence that coronal heating scales with total magnetic flux rather than photospheric magnetic field strength comes from the multi-variable study of Fisher *et al.* (1998). A survey of 333 active regions showed that the X-ray luminosity is more strongly correlated with total flux than with photospheric field strength: once the  $\Phi$  dependence was removed there was no residual correlation with  $B_p$ . Evidence which may contradict this comes from recent studies constructing synthetic coronal images from loop equilibria which use local heating functions depending on the various field-line quantities (Schrijver *et al.*, 2004; Lundquist, 2004). Good matches to observed coronal images seem to require local volumetric heating depending on the footpoint field strength as  $Q \sim B_p/L^2$ . It is possible that this scaling is in fact consistent with (6) or that there is a different scaling for the overall heating than for its distribution within the field.

The Minimum Current Corona model offers one theoretical framework from which we can deduce the value of the reconnection heating constant. A domain composed of field lines of length  $L$ , whose footpoints are moving at  $v_p$ , will be recycled in a time  $\tau_{\text{recyc}} = L/v_p$ . If this recycling occurs as reconnection triggered when the separator current exceeds a threshold, then the value of the threshold should be related to the separator's local magnetic shear,  $I^* \sim LB_c$ , where  $B_c$  is the typical magnetic field strength in the corona. Forming the ratio of these two quantities we find  $I_{\text{qrx}}/\tau_{\text{recyc}} \sim B_c v_p$ . According to the results of Pevtsov *et al.* (2003) the product is approximately constant,  $B_c v_p \simeq 10^5$  G cm/sec, and variations in heating power arise from variations in the flux being reconnected.

Examples we have considered suggest that the field strength at the top of a coronal loop, where reconnection seems to occur, is typically  $B_c \sim 10$  G for a wide range of coronal structures: it is roughly equal in the XBP of 1998 June 17 (at a height of  $\sim 8$  Mm) and in active region AR 9574 (at a height of  $\sim 50$  Mm). The same field value appears as a constant of proportionality,  $P_h/(\Phi v_r) \simeq 10$  G, in surveys of X-ray bright points such as fig. 3. Furthermore, photospheric flux elements of all sizes appear to move at approximately  $v_p \sim 200$  m/sec, typical of the network (the much faster granular velocities are not relevant to this discussion since they move elements too small to influence coronal structure). We propose that it is the product of coronal field and the photospheric velocity,  $B_c v_p \sim 10^5 = 10^6$  Amps/sec, which underlies the observed heating constant. This explanation resembles more traditional scalings from Poynting-flux arguments, except for the critical distinction in the location at which the field strength is estimated. Furthermore, it is possible that a weak dependence on size, through  $\Phi$ , in either  $B_c$ , the X-ray efficiency  $\chi$  or both, leads to the additional  $\Phi^{0.15}$  in the empirical fit of eq. (6).

Quasi-static heating models predict that the slow photospheric motion stores coronal magnetic energy, which is then released by rapid reconnection. There seems to be support in observations and theory for this scenario. For example, the observations of reconnection between AR9574 and AR9570 suggest that reconnection occurs only after a significant period of stressing, and that energy released rapidly by reconnection is dissipated more gradually within the post-reconnection flux. While this sequence offers important insight into the nature of coronal reconnection, and thus into coronal heating, it leaves unanswered some of the key issues. What is the nature of the fast reconnection which is inactive for long periods and then suddenly becomes a fast and effective transported of flux? Once the magnetic energy is released how is it subsequently dissipated? Clearly we are not beginning to understand coronal heating until we know how we might answer these questions.

The author thanks Loren Acton and Alexei Pevtsov for helpful comments during the preparation of the talk and the manuscript. This work was supported by NASA grant NAG5-10489.

## REFERENCES

- Aly, J. J. and Amari, T., *A&A*, vol. 319, 699–719, 1997.
- Aver, E., Longcope, D. W., and Kaneklborg, C. C., *ApJ*, vol. , 2005, (in preparation).
- Baum, P. J. and Bratenahl, A., *Solar Phys.*, vol. 67, 245–258, 1980.
- Biernat, H. K. and Heyn, M. F., *JGR*, vol. 92, 3392–3396, 1987.
- Birn, J., Drake, J. F., Shay, M. A., Rogers, B. N., Denton, R. E., Hesse, M., Kuznetsova, M., Ma, Z. W., Bhattacharjee, A., Otto, A., and Pritchett, P. L., *JGR*, vol. 106, 3715–3720, 2001.
- Biskamp, D., *Phys. Fluids*, vol. 29, 1520–1531, 1986.
- Biskamp, D. and Schwarz, E., *Phys. Plasmas*, vol. 8, 4729–4731, 2001.
- Biskamp, D. and Welter, H., *Phys. Rev. Lett.*, vol. 44, 1069–1072, 1980.
- Cargill, P. J., *ApJ*, vol. 422, 381–393, 1994.
- Close, R. M., Parnell, C. E., Longcope, D. W., and Priest, E. R., *ApJ*, vol. 612, L81–L84, 2004.
- Craig, I. J. D., Henton, S. M., and Rickard, G. J., *A&A*, vol. 267, L39–L41, 1993.
- DeLuca, E. E. and Craig, I. J. D., *ApJ*, vol. 390, 679–686, 1992.
- Erkaev, N. V., Semenov, V. S., and Jamitsky, F., *Phys. Rev. Lett.*, vol. 84, 1455–1458, 2000.
- Fisher, G. H., Longcope, D. W., Metcalf, T. R., and Pevtsov, A. A., *ApJ*, vol. 508, 885–889, 1998.
- Fletcher, L. and Hudson, H., *Solar Phys.*, vol. 204, 69–89, 2001.
- Golub, L., Krieger, A. S., Harvey, J. W., and Vaiana, G. S., *Solar Phys.*, vol. 53, 111–121, 1977.
- Golub, L., Krieger, A. S., Silk, J. K., Timothy, A. F., and Vaiana, G. S., *ApJ*, vol. 189, L93–L97, 1974.
- Gorbachev, V. S., Kelner, S. R., Somov, B. V., and Shvarts, A. S., *Sov. Astron.*, vol. 32, 308–314, 1988.
- Green, R. M., in Lust, R. (ed.), *Stellar and Solar magnetic fields. Proc. IAU Symp. 22*, pp. 398–404, Amsterdam. North-Holland, 1965.
- Greene, J. M., *JGR*, vol. 93, 8583–8590, 1988.
- Hagenaar, H. J., *ApJ*, vol. 555, 448–461, 2001.
- Hagenaar, H. J., Schrijver, C. J., and Title, A. M., *ApJ*, vol. 584, 1107–1119, 2003.
- Heyn, M. and Semenov, V., *Phys. Plasmas*, vol. 3, 2725–2741, 1996.
- Heyvaerts, J. and Priest, E. R., *A&A*, vol. 137, 63–78, 1984.
- Ionson, J. A., *ApJ*, vol. 276, 357–368, 1984.
- Kankelborg, C. C. and Longcope, D. W., *Solar Phys.*, vol. 190, 59–77, 1999.
- Krieger, A. S., Vaiana, G. S., and van Speybroeck, L. P., in Howard, R. (ed.), *Solar Magnetic Fields*, pp. 397–412. IAU, 1971.

- Kulsrud, R. M., *Earth, Planets and Space*, vol. 53, 417–422, 2001.
- Lau, Y.-T. and Finn, J. M., *ApJ*, vol. 350, 672–691, 1990.
- Levine, R. H., *ApJ*, vol. 190, 457–466, 1974.
- Lin, H. and Rimmele, T., *ApJ*, vol. 514, 448–455, 1999.
- Lites, B. W., *ApJ*, vol. 573, 431–444, 2002.
- Longcope, D. W., *Solar Phys.*, vol. 169, 91–121, 1996.
- Longcope, D. W., *ApJ*, vol. 507, 433–442, 1998.
- Longcope, D. W., *Phys. Plasmas*, vol. 8, 5277–5290, 2001.
- Longcope, D. W. and Cowley, S. C., *Phys. Plasmas*, vol. 3, 2885–2897, 1996.
- Longcope, D. W. and Kankelborg, C. C., *Earth, Planets and Space*, vol. 53, 571–576, 2001.
- Longcope, D. W., Kankelborg, C. C., Nelson, J. L., and Pevtsov, A. A., *ApJ*, vol. 553, 429–439, 2001.
- Longcope, D. W. and Klapper, I., *ApJ*, vol. 579, 468–481, 2002.
- Longcope, D. W. and Magara, T., *ApJ*, vol. 608, 1106–1123, 2004.
- Longcope, D. W., McKenzie, D., Cirtain, J., and Scott, J., *ApJ*, vol. , 2005, (submitted).
- Longcope, D. W. and Silva, A. V. R., *Solar Phys.*, vol. 179, 349–377, 1998.
- Lundquist, L., in *Proceedings of SOHO 15*, 2004, (this volume).
- Mandrini, C. H., Démoulin, P., and Klimchuk, J. A., *ApJ*, vol. 530, 999–1015, 2000.
- Nitta, S., Tanuma, S., and Maezawa, K., *ApJ*, vol. 580, 538–549, 2002.
- Parker, E. N., *JGR*, vol. 62, 509–520, 1957.
- Parker, E. N., *ApJ*, vol. 174, 499–510, 1972.
- Parker, E. N., *ApJ*, vol. 330, 474–479, 1988.
- Parnell, C. E., Priest, E. R., and Golub, L., *Solar Phys.*, vol. 151, 57–74, 1994.
- Petschek, H. E., in Hess, W. N. (ed.), *AAS-NASA Symposium on the Physics of Solar Flares*, pp. 425–439, Washington, DC. NASA, 1964.
- Pevtsov, A. A., Fisher, G. H., Acton, L. W., Longcope, D. W., Johns-Krull, C. M., Kankelborg, C. C., and Metcalf, T. R., *ApJ*, vol. 598, 1387–1391, 2003.
- Press, W. H., Flannery, B. P., Teukolsky, S. A., and Vetterling, W. T., *Numerical Recipes: The art of scientific computing*, Cambridge University Press, Cambridge, 1986.
- Rickard, G. J. and Craig, I. J. D., *Phys. Fluids B*, vol. 5, 956–964, 1993.
- Scholer, M. and Roth, D., *JGR*, vol. 92, 3223–3233, 1987.
- Schrijver, C. J., Cote, J., Zwaan, C., and Saar, S. H., *ApJ*, vol. 337, 964–976, 1989.
- Schrijver, C. J., Sandman, A. W., Aschwanden, M. J., and DeRosa, M. L., *ApJ*, vol. , 2004, (in press).
- Schrijver, C. J. and Title, A. M., *ApJ*, vol. 597, L165–L168, 2003.
- Schrijver, C. J., Title, A. M., Van Ballegoijen, A. A., Hagenaar, H. J., and Shine, R. A., *ApJ*, vol. 487, 424–436, 1997.
- Schrijver, C. J. and Zwaan, C., *Solar and Stellar Magnetic Activity*, Cambridge Astrophysics Series. Cambridge University Press, 2000.
- Schrijver, C. J., Zwaan, C., Maxson, C. W., and Noyes, R. W., *A&A*, vol. 149, 123–134, 1985.
- Semenov, V. S., Heyn, M. F., and Kubyshkin, I. V., *Sov. Astron.*, vol. 27, 600–665, 1983.
- Semenov, V. S., Volkonskaya, N. N., and Biernat, H. K., *Phys. Plasmas*, vol. 5, 3242–3248, 1998.
- Sturrock, P. A., Dixon, W. W., Klimchuk, J. A., and Antiochos, S. K., *ApJ*, vol. 356, L31–L34, 1990.
- Sweet, P. A., in Lehnert, B. (ed.), *Electromagnetic Phenomena in Cosmical Physics*, pp. 123–134. Cambridge University Press, Cambridge, U.K., 1958a.
- Sweet, P. A., *Nuovo Cimento*, vol. 8, 188–196, 1958b.
- Syrovatskii, S. I., *Sov. Phys. JETP*, vol. 33, 933–940, 1971.
- Taylor, J. B., *Phys. Rev. Lett.*, vol. 33, 1139–1141, 1974.
- Tucker, W. H., *ApJ*, vol. 186, 285–289, 1973.
- Ugai, M. and Tsuda, T., *J. Plasma Phys.*, vol. 17, 337–356, 1977.
- Van Ballegoijen, A. A., *ApJ*, vol. 298, 421–430, 1985.
- Withbroe, G. L. and Noyes, R. W., *ARA&A*, vol. 15, 363–387, 1977.